SL9 Impact Imaging, Spectroscopy, and Long–Term Monitoring from the Calar Alto Observatory

T. M. Herbst[1], D. P. Hamilton[2], H. Böhnhardt[3], and J.L. Ortiz–Moreno[4]

[1] Max-Planck-Institut für Astronomie, Heidelberg; [2] Max-Planck-Institut für Kernphysik, Heidelberg;
[3] Universitäts–Sternwarte, München; [4] Instituto de Astrofisica de Andalucia, Granada

Abstract: We present several early results from the Calar Alto program of near infrared imaging and spectroscopy of the collision of Comet Shoemaker–Levy 9 with Jupiter. Observations and timing of seven separate impacts indicate that the precursors are ubiquitous and associated with phenomena at or near the time of atmospheric entry. The impact of the Q2 fragment was very unusual in having a precursor brighter than the main event. Strong CO emission in K band spectra taken near maximum light of the H impact indicate temperatures above 2000 K. Finally, monitoring of the disk of Jupiter in the seven months since the collision show longitudinal spreading of the impact structures at approximately 10 m s^{-1}, with very little spreading in latitude.

Introduction and Observations

We observed ten separate impacts using the MAGIC infrared camera mounted at the Ritchey–Chrétien focus of the 3.5 meter telescope on Calar Alto. MAGIC contains a 256×256 HgCdTe detector array originally developed for the Space Telescope NICMOS program. This detector is sensitive from $\lesssim$1 to 2.5 μm, and in combination with various filters and grisms, allows imaging and spectroscopy in the J, (1.13–1.37 μm), H (1.5–1.8 μm), and K (2.0–2.4 μm) photometric bands. Most of the observations presented here used a custom filter set from Omega Optical (J. Spencer, 1994 personal communication). One of these filters, centered at 2.3 μm, isolates a spectral region where absorption from methane in the Jovian atmosphere darkens the cloud deck and enhances the contrast of the impact structures. We used a direct–ruled ZnSe grism for the spectroscopic measurements. This device gives complete K band coverage with spectral resolution $\frac{\lambda}{\Delta\lambda} \sim 360$ in a single exposure. Herbst *et al.* (1993, 1994, 1995) describe the MAGIC camera and these observations in detail.

Precursor Timing and the Q2 Impact

Table 1 summarizes the timing of the seven impacts we detected from Calar Alto. The primary result of these observations is that *all the impact measurements with high signal–to–noise ratio show distinct precursor events, and in every instance, the precursor occurs at the accepted impact time.* This indicates that the precursors are associated with phenomena at or near the time of entry of the fragment into the Jovian atmosphere. The"main event" or maximum light takes place some 5 to 8 minutes later.

The impact of the Q2 fragment was unique among all the events observed in having a short–lived precursor flash that was brighter than the main event itself (Figure 1). More typically, the main event was tens to hundreds of times brighter than the precursor. The Q2 impact was also unusual in having a delay between the precursor and main event approximately 1–2 minutes longer than the other impacts. Q2 was also one of the few "off–line" fragments prior to impact. In a companion paper presented at this conference, Hamilton *et al.* argue on the basis of our H and L impact observations that two separate precursor events occur, the first associated with the meteor flash of entry, and the second, brighter one approximately a minute later, corresponding to the plume travelling back up the evacuated entry channel (see also Hamilton *et al.* 1995). This picture provides a natural explanation for the bright Q2 precursor and the longer delay time until the main event. Perhaps the Q2 fragment was not very solid: poor structural integrity would cause the impactor to "pancake" high in the atmosphere, depositing a significant fraction of its energy on entry, and leading to a relatively small main event almost eight minutes later. In other words, the Q2 fragment produced only a first "bolide" precursor.

Impact	Date	Accepted Impact Time	Start of Precursor	Start of Main Event	Precursor–Main Δt
A	16 July	20:11 ± 3	20:11:29 ± 5	20:16:56 ± 5	5.4 min
E	17 July	15:11 ± 3	–	15:17:56 ± 5	–
H	18 July	19:32 ± 1	19:31:45 ± 20	19:37:27 ± 15	5.7 min
L	19 July	22:17 ± 1	22:16:18 ± 3	–	–
P2	20 July	15:23 ± 7	nd	nd	–
Q1	20 July	20:12 ±4	20:13:15 ± 5	20:19:47 ± 5	6.5 min
Q2	20 July	19:44 ± 6	19:44:47 ± 3	19:52:24 ± 15	7.6 min
S	21 July	15:15 ± 5	–	15:22 ± 2	–
T	21 July	18:10 ± 7	nd	nd	–
U	21 July	21:55 ± 7	nd	nd	–

Table 1 Summary of the Calar Alto impact observations and timing (nd means not detected). We saw precursors close to the accepted impact times in all instances with good signal to noise ratio. Instrument problems prevented our observing any possible S precursor, and the E event took place during poor, daytime conditions in Spain.

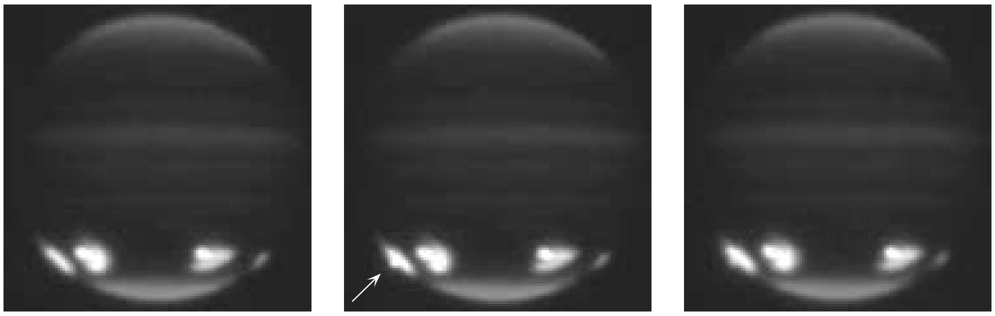

Figure 1 Jupiter just prior to the Q2 impact (left), the Q2 precursor (center), and the main event (right). The precursor of the Q2 fragment impact was brighter than the main event. All three images taken on 20 July 1994 in the 2.3 μm absorption band of methane.

CO Spectroscopy

Figure 2 shows a sequence of K band spectra of the H impact taken over a six minute time span near maximum light. Deep absorption features due to molecular hydrogen (2.12 μm) and CH_4 (2.3 μm) darken the planet at these wavelengths. Rapidly–evolving emission features due to the $\Delta v = 2$ bandhead transitions of carbon monoxide dominate the spectrum longward of 2.3 μm. The CO bandheads consist of more than 700 individual lines which are unresolved in these measurements. CO bandhead emission is a diagnostic of warm, molecular gas with excitation temperatures in the range 2000–5000 K. At lower temperatures, the higher order bandheads are not excited, while at higher temperatures, the CO dissociates (Scoville *et al.* 1983; Carr 1989).

We have begun modelling these spectral features in order to reveal the physical conditions in the emitting regions. Following the lead of Scoville *et al.* (1983), we calculate synthetic spectra as a function of excitation temperature, the optical depth in a single transition at the $v = 2 - 0$ bandhead, and the velocity width of the (assumed) Gaussian line profile. Under LTE conditions, the emission spectrum is then $I_\lambda = B_\lambda(T) \cdot (1 - e^{-\tau(\lambda)})$, where B_λ is the Planck function and

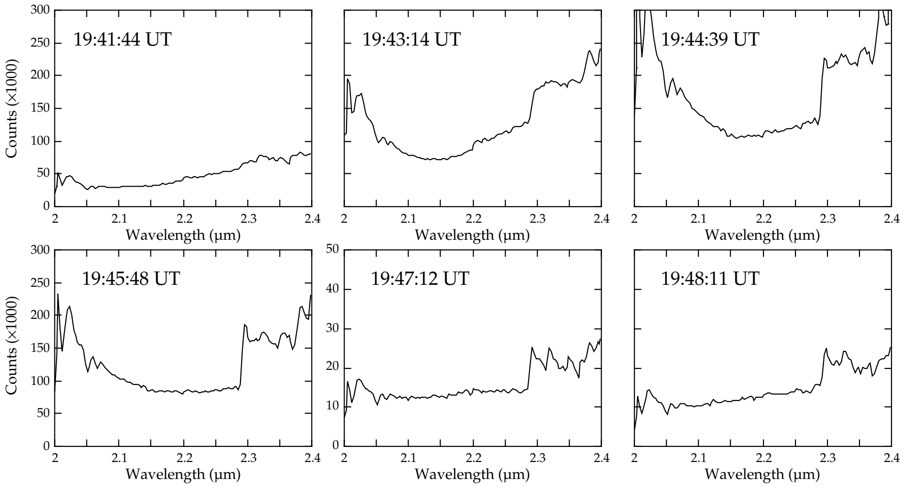

Figure 2 K band spectra near maximum light of the H impact on 18 July 1994.

the optical depth $\tau(\lambda)$ is summed over all transitions within a few velocity widths of λ. At this writing, the modeling process is not complete, but early trials indicate high temperatures ($\sim$3000 K) and larger optical depths near maximum light, with both values dropping as the main event fades. The models are relatively insensitive to the width of the individual emission lines at this spectral resolution. Figure 3 shows a sample fit for the spectrum at 19:47:12 in Figure 2. The disappearance of the third, $v = 4 - 2$ bandhead in the subsequent spectrum argues for a temperature drop of a few hundred degrees in the intervening minute.

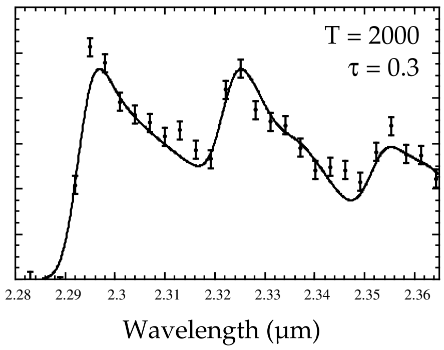

Figure 3 (left) Sample fit (solid line) to the CO spectrum measurements (points) taken during the H impact at 19:47:12 on the 18th of July. This combination of parameters reproduces the relative strengths and shapes of the first three bandheads seen in the observations.

These models are a necessary first step in understanding the complex impact phenomena, but they have significant shortcomings. First, it is unlikely that the emitting gas is in LTE as the model assumes. While the relatively high densities of planetary atmospheres would encourage LTE conditions relative to astrophysical environments, there are undoubtedly other ongoing processes, such as shocks and molecule formation, which complicate the picture. In addition, the emitting slab model assumes a single temperature, which is almost certainly not the case. The dramatic change in the spectra between 19:45:48 and 19:47:12 (Figure 2) indicates a significant change in temperature and optical depth. The automatic data acquisition program nodded the telescope at this time, perhaps displacing the slit somewhat and thereby sampling a slightly different portion (and temperature) of the emitting gas. Clearly, disentangling all these effects will be difficult.

Long Term Monitoring

Although this paper appears in the "Fireballs and Plumes" session, the Calar Alto observing program by no means ended during the plume phase of the impacts. We have been monitoring the evolution of the impact structures in the months since last July, and the changes on Jupiter are remarkable. Figure 4 shows the planet three days (left), one month (center) and seven months (right) after the last of the impacts (the last image was taken 36 hours after this conference

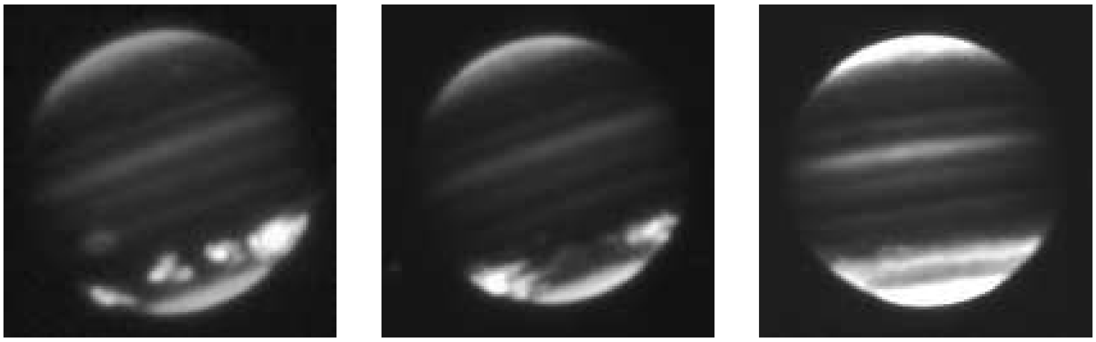

Figure 4 The impact sites on Jupiter 3 days (left), one month (center), and seven months (right) after the last fragment of Comet Shoemaker–Levy 9 struck the planet. The impact structures now form a continuous band in Jupiter's southern hemisphere. All images taken in the 2.3 μm absorption band of methane.

ended).

Considerable spreading of the impact sites took place in the ten weeks following the collision, and the impact structures now form a continuous band encircling the southern hemisphere of Jupiter. The sites have also faded somewhat, requiring a "harder" intensity stretch in the righmost frame. Identifying the individual features in these and other images with their parent impact sites allows an estimate of the rate of longitudinal spreading. This rate is in the range 1.2–1.5° per day, or 10–14 m s^{-1}. The band in the rightmost image in Figure 4 is not significantly wider than the original impact sites in July (leftmost image). Allowing a maximum latitudinal growth of 10,000 km (Jupiter's diameter is 140,000 km) gives an upper limit to the north–south spreading of $\sim$0.5 m s^{-1}.

Conclusions

This short paper has touched on several unrelated aspects of a large observational data set. Any conference for which the cover of the abstract booklet shows an image less than two weeks old must necessarily involve work in progress, and our observations are no exception. Nevertheless, the near infrared imaging and spectroscopy from Calar Alto and elsewhere have proven very useful in unravelling these complex impact phenomena.

T. H. is grateful to John Carr for updated molecular constants and for useful discussions on the physics of CO emission.

References

Carr, J. S. (1989), *Ap. J.*, **345**, 522.
Hamilton, D. P., Herbst, T. M., Böhnhardt, H.,Ortiz–Moreno, J–L, 1995. GRL, submitted.
Herbst, T. M., Hamilton, D. P., Böhnhardt, H.,Ortiz–Moreno, J–L, 1995. GRL, submitted.
Herbst, T. M., and Rayner, J. T., (1994) in "Infrared Arrays: The Next Generation," Kluwer, page 515.
Herbst, T. M., Beckwith, S. V. W., Birk, Ch., Hippler, S., McCaughrean, M. J., Mannucci, F., and Wolf, J., (1993) in "Infrared Detectors and Instrumentation," SPIE Technical Conference 1946, page 605.
Scoville, N., Kleinmann, S. G., Hall, D. N. B., and Ridgway, S. T., (1983), *Ap. J.*, **275**, 201.